Electronic Supplementary Material (ESI) for Journal of Materials Chemistry C.
This journal is © The Royal Society of Chemistry 2015

Electronic supplementary information (ESI) for

Defect Trapping States and Charge Carrier Recombination in Organic-Inorganic Halide Perovskites

Xiaoming Wen, [a]* † *Yu Feng,* [a] † *Shujuan Huang,*[a] *Fuzhi Huang,*[b] *Yi-Bing Cheng,*[b] *Martin Green*[a] *Anita Ho-Baillie*[a]

[a] Australian Centre for Advanced Photovoltaics, University of New South Wales, Sydney 2052, Australia;

[b] Department of Materials Engineering, Monash University, Victoria 3800, Australia

Keyword: perovskite, defect trapping, saturation

Corresponding author: X W x.wen@unsw.edu.au

†: X Wen and Y Feng contributed equally to this work.

Experimental Section

Material synthesis and precursor preparation:

Unless specified otherwise, all materials were purchased from either Alfa Aesar or Sigma-Aldrich and used as received. CH_3NH_3I was synthesized by mixing 24 mL CH_3NH_2 (33% in ethanol) and 10 mL HI (57% in water) in 100 mL ethanol. After stirring for 2h, the solvent was removed on a rotary evaporator. The white crystals were dried in a vacuum oven at 60 ºC for 24h.

Sample for spectroscopy

The soda-lime glass substrates were cleaned and then cut into around 1 cm^2. A 25µL 45wt% $CH_3NH_3PbI_3$ DMF solution, prepared from PbI_2 and CH_3NH_3I in a molar ratio of 1:1, was spread on it, on a spin-coater. For the conventional spin-coating method, the solution was spun at 6500 rpm for 30 s, while for the gas-assisted method, a 40 psi dry Argon gas stream was blown over the film during spinning at 6500 rpm in 2 s after the spin-coating commenced. The films were then annealed at 100 ºC on a hotplate for 10 min, and then cooled to room temperature on a steel substrate.

Spectroscopic measurements

The low excitation PL lifetime was performed using TCSPC in a Fluoromax-4 spectrofluorimeter with 470 nm excitation with repetition of 2 MHz. The PL time traces and PL decay traces were measured in Microtime200 (Picoquant) with excitation of 470 nm laser. The time resolution of the system was determined by measuring the response function of the laser pulse, as 150 ps. At high excitation intensity, the PL intensity at detector was attenuated suitably for single photon counting. The experiment was undertaken at room temperature.

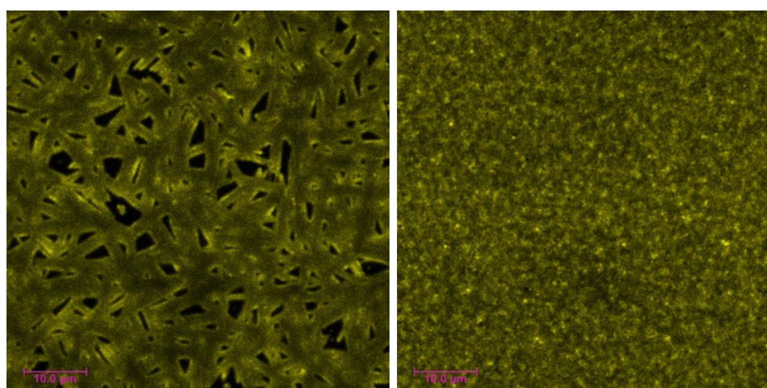

Fig. S1 Morphology of (a) SC and (b) GA samples by fluorescence imaging.

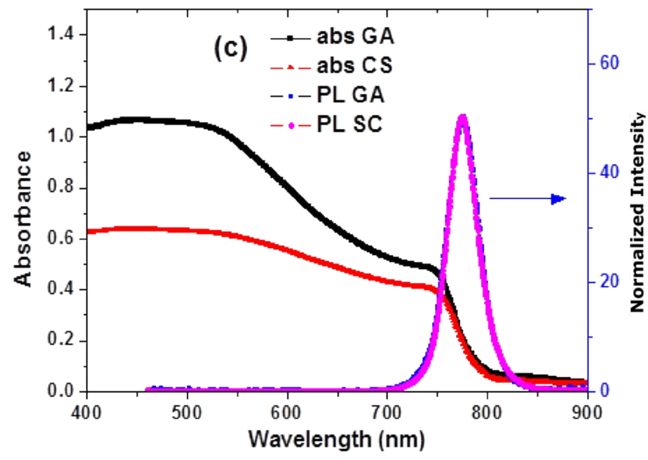

Fig. S2 absorption and PL spectra of SC and GA samples.

Modelling

To model the relation between the steady state PL intensity and the excitation intensity, we assume two recombination mechanisms are dominant, including the band-to-band recombination and SRH recombination via shallow defect trap states. Without lack of generality, we further assume the trapping states sit at a single energy level close to the conduction-band edge (Fig.3).[1-2] In this case, the process of electrons being trapped into theses states (trapping) is much faster than the process of trapped electrons being relaxed to the valence band (desaturation). The reason is that the carrier depopulation relies on the assistance of multi-phonon emission, which is regarded as a higher order perturbative process and happens much more rarely according to the perturbation theory.

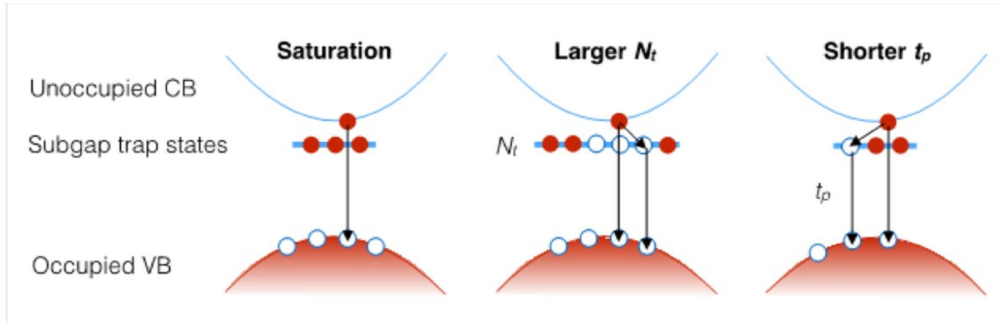

Fig.S3 Saturation of the subgap trap states and desaturation by either increasing the trap-state density N_t or reducing the depopulation lifetime t_p

The rate of electrons being trapped by the defect states and the rate of defect states being depopulation and relaxing trapped electrons to the valence band are expressed respectively by

$$R_n = \left[n(1 - f_t) - N_i e^{\beta\Delta} f_t\right]/t_n \tag{1}$$

$$R_p = \left[p f_t - N_i e^{-\beta\Delta}(1 - f_t)\right]/t_p \tag{2}$$

where $\Delta = E_t - E_i$ is the energy difference between the trap state energy level E_t and the material's intrinsic (i.e. undoped) Fermi level E_i. n and p are the concentrations of free electrons and holes, respectively. f_t denotes the occupation probability of the shallow defect states ($0 \le f_t \le 1$), and N_i is the material's intrinsic carrier concentration. The lifetimes of the saturation and the depopulation processes are denoted by t_n and t_p respectively. According to our assumption, $t_n \ll t_p$. At steady state a balance is established between the saturation and depopulation processes, i.e. $R_n = R_p$. After algebraic manipulation this condition leads to

$$f_t = \frac{1/t_n + N_i e^{-\beta\Delta}/t_p}{\left(n + N_i e^{\beta\Delta}\right)/t_n + \left(p + N_i e^{-\beta\Delta}\right)/t_p} \tag{3}$$

The conservation of the total number of electron gives $n + N_t f_t - p = C$, where N_t denotes the concentration and the shallow defect states, and the constant C stands for the density of electrons contributed by the trap states. For typical electron acceptor $C = 0$, while for typical electron donor $C = N_t$. After applying the conservation condition, Eq. 3 is transformed to a quadratic equation:

$$t_n N_t f_t^2 + \left[t_n\left(n + n_i e^{-\beta\Delta} - C\right) + t_p\left(n + n_i e^{\beta\Delta}\right)\right] f_t - \left(t_n n_i e^{-\beta\Delta} + t_p n\right) = 0 \tag{4}$$

Here we assume that the shallow defect states close to conduction band edge is of electron acceptor type ($C = 0$), which is consistent with literature work.[3] In fact, if the defect states act as electron donors, they are close to complete saturation even at low injection levels thus violating the observed phenomena that the defect state are gradually saturated when increasing the injection level.

At relatively high injection levels (excitation intensity $\gtrsim$ 500 mW/cm^2), the subgap states tend to be filled. This means that the quasi-Fermi level of electrons reaches the defect energy level implying $n \gtrsim n_i e^{\beta\Delta}$. This allows us to approximate Eq.4 to

$$t_n N_t f_t^2 + t_p n f_t - t_p n = 0\,. \tag{5}$$

Within the range of the injection levels in the conducted steady state PL experiments (excitation intensity $\lesssim$ 5000 mW/cm^2), the free electron concentration is not sufficiently high compared to the large defect state density. We can further impose an assumption that $N_t \gtrsim n t_p / t_n$. It is noted that all the assumptions will be further validated by the numerical results retrieved from the experimental data. Under these assumptions, an approximate solution for Eq. 5 is

$$f_t = \frac{\sqrt{n t_p}}{\sqrt{n t_p} + \sqrt{N_t t_n}} \tag{6}$$

An amazing thing is that the approximate solution no longer depends on the uncertain defect energy level E_t. It allows f_t to vary between 0 and 1 depending on the ratio of $n t_p$ to $N_t t_n$. Substituting this expression for f_t and the electron conservation condition into Eq.1 or Eq.2, the rate of shallow subgap state SRH recombination is expressed as a function of the free electron concentration n:

$$R(n) = \frac{1}{t_p + t_n n + \sqrt{N_2}\, n^{1/2} + N_2} \frac{\left(\sqrt{N_1 N_2} - N_2\right) n}{} + \frac{n}{t_p + t_n} \tag{7}$$

The definitions of N_1 and N_2 are

$$N_1 = N_t t_p / t_n,\; N_2 \approx N_t t_p t_n / (t_p + t_n)^2 \approx N_t t_n / t_p \tag{8}$$

The assumption that $t_n \ll t_p$ leads to the inequality $N_1 \gg N_2$. It is thereby a reasonable approximation to replace $\sqrt{N_1 N_2} - N_2$ by $\sqrt{N_1 N_2}$ and neglect the second term in Eq. 7:

$$R(n) \approx \frac{\sqrt{N_1N_2}}{t_p + t_n n + \sqrt{N_2}n^{1/2} + N_2} n. \tag{9}$$

Other than the SRH recombination via the trapping states, we suppose the only carrier decay path is via band-to-band recombination whose rate is proportional to the product of n and p. In fact, the band-to-band recombination takes the dominant role at high injection levels due to the saturation of defect trap states. Its recombination rate r, as a function of the free electron concentration n, is proportional to the product of respective free carrier concentrations:

$$r(n) = \beta np \approx \beta n N_t f_t \approx \frac{\beta\sqrt{N_1N_2}}{n^{1/2} + \sqrt{N_2}} n^{3/2} \tag{10}$$

Where β is the rate coefficient of the band-to-band recombination. The first approximation in Eq.10 is because that the free carrier concentration is relatively low compared to the trapped electrons at the injection levels of the experiments. The second approximation is directly from Eq.6 and Eq.8.

It is noted that the band-to-band recombination rate $r(n)$ determines the PL intensity I_{pl}. As the absolute value of the PL intensity does not have any physical meaning, we normalized the intensity to its maximum value ensuring $0 < I_{pl} \leq 1$. According to Eq.10, I_{pl} can be expressed by

$$I_{pl} = \frac{1 + \sqrt{N_2/n_m}}{(n/n_m)^{1/2} + \sqrt{N_2/n_m}} (n/n_m)^{3/2} \tag{11}$$

Where n_m is the maximum value of the free electron concentration n, or equivalently the electron concentration at the maximum excitation intensity of the experiment.

If assuming that the absorbed photons are completely utilised to generate electron-hole pairs, and that the annihilation of electron-hole pairs is due to either defect state tapping or band-to-band recombination, then a balance equation can be written

$$G = R(n) + r(n) \approx \frac{\sqrt{N_1N_2}}{t_p + t_n} \frac{\hat{n}}{\hat{n} + \sqrt{\frac{N_2}{n_m}}\hat{n}^{\frac{1}{2}} + \frac{N_2}{n_m}} + \frac{\beta n_m \sqrt{N_1N_2}}{\hat{n}^{1/2} + \sqrt{\frac{N_2}{n_m}}} \hat{n}^{3/2} \tag{12}$$

It is noted that when substituting Eq.9 and Eq.10 inot Eq.12, we use the normalised value $\hat{n} = n/n_m$ for the free electron density instead of its absolute value. The average rate of photocarrier generation is

$$G = \frac{1 - e^{-\alpha d}}{d} \frac{I_{ex}}{E_{ph}}. \tag{13}$$

Eq.12 can be further simplified by defining three parameters a_1, a_2 and a_3:

$$\frac{1-e^{-\alpha d}}{d}\frac{I_{ex}}{E_{ph}}=\frac{a_1\hat{n}}{\hat{n}+a_3\hat{n}^{1/2}+a_3^2}+\frac{a_2\hat{n}^{3/2}}{\hat{n}^{1/2}+a_3}, \tag{14}$$

where

$$a_1=\frac{\sqrt{N_1N_2}}{t_p+t_n}, \tag{15}$$

$$a_2=\beta n_m\sqrt{N_1N_2}, \tag{16}$$

$$a_3=\sqrt{N_2/n_m}. \tag{17}$$

According to Eq.11, the normalized electron density $\hat{n}$ can be expressed as a function of the normalized PL intensity I_{pl}:

$$\sqrt{\hat{n}(I_{pl})}=\frac{I_{pl}}{(3+3a_3)}\left[\frac{I_{pl}}{2a_3^{-1}+2}-\sqrt{\frac{I_{pl}^2}{(2a_3^{-1}+2)^2}-\frac{I_{pl}^3}{(3+3a_3)^3}}\right]^{-\frac{1}{3}}+\frac{I_{pl}}{(3+3a_3)}\left[\frac{I_{pl}}{2a_3^{-1}+2}+\sqrt{\frac{I_{pl}^2}{(2a_3^{-1}+2)^2}-\frac{I_{pl}^3}{(3+3a_3)^3}}\right]^{-\frac{1}{3}}. \tag{18}$$

Eq.14 combined with Eq.18 describes the relation between the excitation intensity I_{ex} and the steady state PL intensity I_{pl}, thus leading to a trivariate fitting. The three variables a_1, a_2 and a_3 that are obtained from fitting can be used to derive physical parameters related to the trap-state property of the investigated material:

$$\frac{N_t}{t_p}\approx\frac{N_t}{t_p+t_n}\frac{t_p}{t_p+t_n}=a_1, \tag{19}$$

$$\frac{n_m}{t_n}\approx\frac{n_m}{t_n}\frac{t_p}{t_p+t_n}=\frac{a_1}{a_3^2}. \tag{20}$$

If supposing the band-to-band recombination is purely radiative, the radiative quantum yield is calculated using:

$$\eta(n)=1-\frac{R(n)}{G}. \tag{21}$$

where the SRH recombination rate $R(n)$ is given by Eq.7 and the total photocarrier generation/recombination rate is provided by Eq.13.

Table 1: Determination of N_t, n_m, t_p, and t_n using fitted results and published values of R_{pop} and R_{dep}

Sample	Literature constants		Combined with fitted results			
	R_{pop}	R_{dep}	N_t (cm^{-3})	n_m (cm^{-3})	t_p (s)	t_n (s)

	(cm^3/s)	(cm^3/s)				
SC	2.00×10^{-10}	8.00×10^{-12}	7.44×10^{16}	6.51×10^{16}	1.68×10^{-6}	6.72×10^{-8}
GA			1.04×10^{17}	1.24×10^{17}	1.20×10^{-6}	4.82×10^{-8}

For both samples, the assumption $t_p \gg t_n$ is consistent with the fitting results shown in Table.1. Despite that at the maximum excitation intensity $N_t < n_m t_p/t_n$, the assumption $N_t \gtrsim n t_p/t_n$ is still valid for most of the data points at excitation intensities below 5000 mW/cm^2. This validates the assumptions adopted in this model. Another assumption that $n \gtrsim n_i e^{\beta\Delta}$ is valid as long as the trap state energy level is below the conduction band edge by at least several thermal smearing energies (*kT*). Although this assumption is not possible to be validated using the experiment technique here, it is not a tight assumption at all. Considering the limitation of the steady state photoluminescence, the model greatly improves its ability of characterising defect state properties of fabricated perovskite samples.

1. Yin, W.-J.; Shi, T.; Yan, Y., Unusual defect physics in CH3NH3PbI3 perovskite solar cell absorber. *Appl. Phys. Lett.* **2014,** *104* (6), 063903.
2. Yin, W.-J.; Shi, T.; Yan, Y., Unique properties of halide perovskites as possible origins of the superior solar cell performance. *Adv. Mater.* **2014,** *26* (27), 4653-8.
3. Stranks, S. D.; Burlakov, V. M.; Leijtens, T.; Ball, J. M.; Goriely, A.; Snaith, H. J., Recombination Kinetics in Organic-Inorganic Perovskites: Excitons, Free Charge, and Subgap States. *Phys. Rev. Appl.* **2014,** *2* (3), 034007.